Polarization-independent long-wavelength cut off filter with symmetrical film system

SHIFU XIONG, XIUHUA FU*, YUSHUAI ZHANG, JING ZHANG
School of Photo-Electronic Engineering, Changchun University of Science and Technology, Changchun 130022, China

In this paper, a new kind of symmetrical film structure (αLHαL) was proposed to design polarization-independent long-wavelength cutoff filter for optical-fiber communication system. The system consists of films without thinner films (<30nm) which is suitable for accurately monitoring with the indirect monochromatic optical monitor technique. The prepared filter achieved excellent optical propagation characteristic corresponds to the theoretical spectral performance. The experimental result demonstrates that it realizes zero separation of p- and s-polarization and possesses high and smooth transmission curve in the transmission region. Moreover, polarization-independent filters at different incident angles can be achieved just according to adjusting the value of α.

(Received December 26, 2016; accepted June 7, 2017)

Keywords: Thin films, Multilayer design, Depolarization, Long-wavelength cut off filter

1. Introduction

Optical thin film coating is becoming increasingly significant in industrial processes. The cutoff filter based on film system is widely used in optical instruments which can be passed through by light in specified wavelength region [1]. A cutoff filter with an ideal performance will have higher transmission and reflectance in the transmission and cut-off region respectively. In addition, the boundary between the transmission and cut-off region is steeper, the performance of the filter is better.

Unfortunately, the separation of p- and s-polarization components of light always affects the performance of cutoff filters in the case of oblique incidence, especially for an optical-fiber communication. To overcome this problem, several design approaches of polarization-independent cutoff filter have been reported in these papers [2~5]. According to this survey results, the biggest challenge is how to achieve depolarization. The filter also should possess higher and smoother transmission curve in transmission region, and higher reflectivity in cut-off region.

In this paper, a novel and compact polarization-independent long-wavelength cutoff filter based on a special symmetrical film system structure is proposed, which is designed by using the commercial software TFCalc. This design can achieve zero separation between the two polarization components.

2. Design of the filter

As shown in Table 1, the substrate(short for sub in the following) glass is BK7 and the incident medium is air. The main requirement parameters of the filter have been given in Table 1.

Table 1. The specifications of the on-polarized filter

Parameters	Specifications
Incident angle/°	30±1.2
Pass band/nm	850±10
Reflection band/nm	908±8
Transmission (p & s) of pass band/%	≥95
Reflectance (p & s) of reflect band/%	≥99

Ta_2O_5 and SiO_2 dielectric thin films have great advantages in the applications of optical communication technology because of their excellent transparency, environmental stabilities, and refractive index difference[6]. Therefore, Ta_2O_5 and SiO_2 were still used as design materials in this paper, which of the refractive index are 2.12 and 1.46 respectively.

The proposed cutoff filter includes quarter-wave layers with high and low refractive, which is donated as H and L respectively. The basic structure is sub|(αLHαL)^s|air, s is the period number, α represents correction factor which is used to adjust the thickness of the detuned outer layers. The symmetrical stack forms the basis structure of this filter, which of transmission character can be described by a transmission matrix. The matrix is as follow:

$$M=\begin{bmatrix} m_{11} & m_{12} \\ m_{21} & m_{22} \end{bmatrix}=\begin{bmatrix} \cos\delta_L & \frac{i}{\eta_L}\sin\delta_L \\ i\eta_L\sin\delta_L & \cos\delta_L \end{bmatrix}\begin{bmatrix} \cos\delta_H & \frac{i}{\eta_L}\sin\delta_H \\ i\eta_H\sin\delta_H & \cos\delta_H \end{bmatrix}\begin{bmatrix} \cos\delta_L & \frac{i}{\eta_L}\sin\delta_L \\ i\eta_L\sin\delta_L & \cos\delta_L \end{bmatrix} \quad (1)$$

In which δ is phase thickness. So that,

$$m_{11}=m_{22}=\cos(2\delta_L)\cos\delta_H-\frac{1}{2}\left(\frac{\eta_H}{\eta_L}+\frac{\eta_L}{\eta_H}\right)\sin(2\delta_L)\sin\delta_H$$
$$=\cos\left(2\cdot\frac{\pi}{2}g\alpha\right)\cos\left(\frac{\pi}{2}g\right)-\frac{1}{2}\left(\frac{\eta_H}{\eta_L}+\frac{\eta_L}{\eta_H}\right)\sin\left(2\cdot\frac{\pi}{2}g\alpha\right)\sin\left(\frac{\pi}{2}g\right) \quad (2)$$

Where $g=\lambda_0/\lambda$, $\eta_H=n_H/\cos\theta_H$ and $\eta_L=n_L/\cos\theta_L$ for p-polarization, $\eta_H=n_H\cos\theta_H$ and $\eta_L=n_L\cos\theta_L$ for s-polarization, θ_H and θ_L are the angle of refraction in high and low index layers. The edge of the pass band was determined by

$$m_{11}=m_{22}=\pm1 \quad (3)$$

With $m_{11}=m_{22}=-1$, $\rho=\eta_H/\eta_L$, then

$$\frac{\rho+\frac{1}{\rho}-2}{\rho+\frac{1}{\rho}+2}=\frac{\cos^2\left[\frac{\pi}{2}g\left(\frac{2\alpha+1}{2}\right)\right]}{\cos^2\left[\frac{\pi}{2}g\left(\frac{2\alpha-1}{2}\right)\right]} \quad (4)$$

$$\rho_P=\left(\frac{\eta_H}{\eta_L}\right)_P=\frac{n_H\cos\theta_L}{n_L\cos\theta_H}$$
$$\rho_S=\left(\frac{\eta_H}{\eta_L}\right)_S=\frac{n_H\cos\theta_H}{n_L\cos\theta_L} \quad (5)$$

Where g_p and g_s are the band edge of p- and s-polarization, respectively. That is, the separation of p- and s-polarization can be expressed as

$$\delta_g=g_S-g_P \quad (6)$$

Based on the above analysis, using equation (6) to evaluate the separation of p- and s-polarization and the polarization effect.

With s=29, it can be seen from Table 2 and Fig. 1. As increasing the value of α, the separation of p- and s-polarization is decreasing, and the same to reflection band. When α=0.5 or 1, many deep ripples appear in the transition region. Then continuously increasing α, the filter will achieve better performance when α=1.5. However, if α is bigger than 1.5, such as 2.0, many ripples will appear in the transmission band due to the mismatching of the equivalent admittance of substrate, the multilayer stack and the incident medium. At the same time, the reflection band decrease rapidly, which will seriously affect the performance of the filter. In addition, when the thickness of Ta_2O_5 and SiO_2 layers are close, the film system will be more easily to fabricate.

Table 2. The polarized separation with different structure

α	0.5	1	1.5	2
δ_g	2.11×10^{-2}	1.42×10^{-2}	0.65×10^{-2}	0.36×10^{-2}
Width of rejection /nm	217	85.9	45.15	27.6

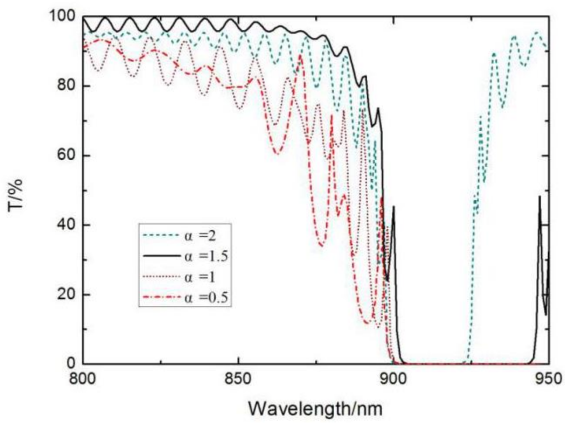

Fig. 1. The average light transmission curves of the special structure of sub|(αLHαL)^s|air with different value of α when the incidence angle is 30 degrees

Depending on the previous discussion, take all factors into account, when α=1.2, and the matching layers between stack and substrate are increased, the theory design will realize better performance. In addition, using high refractive index material Ta_2O_5 as the first layer will contribute to decrease the stress between the film and substrate, and it also benefits a more stable deposition rate than SiO_2. Therefore, the long-wavelength cutoff filter include sub|H(1.2LH1.2L)^29 HL|air can achieve better performance. However, it is necessary to optimize the layer thickness to reduce ripples in the transmission band.

It is well known that needle synthesis is an easy and effective method to optimize the film, which has been illustrated in other papers [7~8]. However, using this method will generate thinner layers that is difficult to control in the process of deposition. In this paper, the commercial software TFCalc is used to optimize the film system. Variable metric and constrained optimization method with low and high constrains for layers thickness were used, and the upper and lower constrains for layer physical thicknesses are 250 nm and 50 nm.

The theoretical transmission curves of average light, p- and s-polarization light with 62-layers designed at the incident angle of 28.8˚, 30˚ and 31.2˚ were shown in Fig. 2(a), (b) and (c). It can be seen that the design realizes zero separation between two polarization components and ripples in the transmission band has been suppressed effectively. The curve is very smooth in the whole transmission band and the reflection band is flat. Fig. 2(d) shows the transmission curve for average light at 28.8˚, 30˚ and 31.2˚. The main effect of increasing the incident angle is that the transmission curve moves to shorter wavelengths. When the incident angle from 28.8˚ to 31.2˚, the transmission curve moves to shorter wavelength approximately 6 nm.

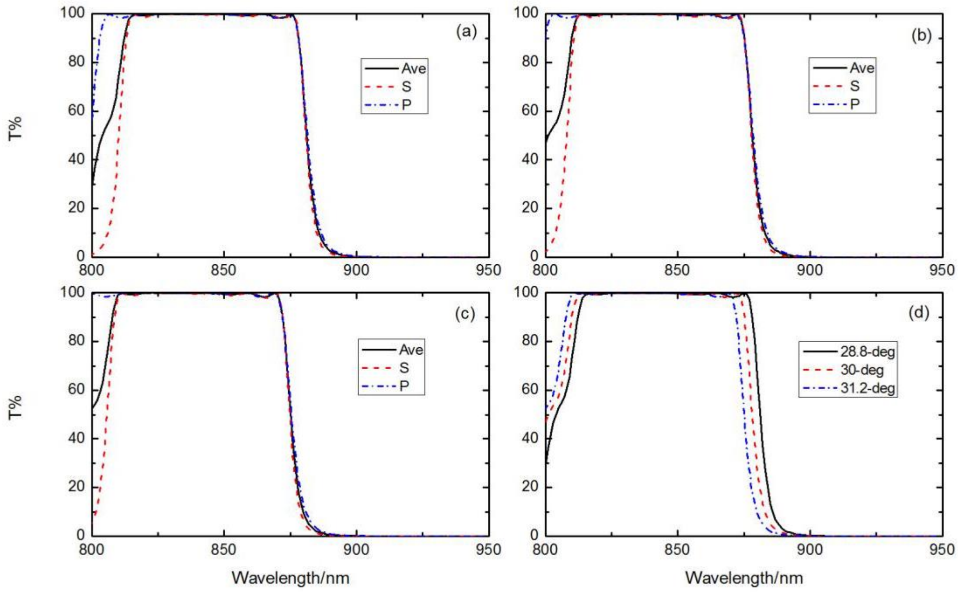

Fig. 2. (a), (b) and (c) show the transmission curves of average light, p- and s-polarization components with the 62-layers design at the incident angle of 28.8˚, 30˚ and 31.2˚, and (d) shows the average light transmission curve at the incident angle of 28.8˚, 30˚ and 31.2˚

Fig. 3 gives the thickness distribution graph of the filter. The total physical thickness is 6.3 μm, and the minimum and maximum layer thickness is 56.5 nm and 190.5 nm. Therefore, the layer thickness can reach more evenness by using constrained optimization method, and the film is easier to fabricate.

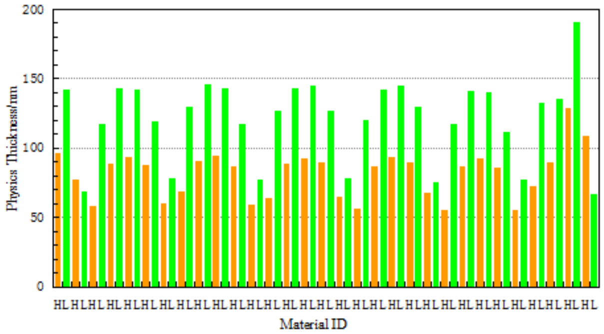

Fig. 3. Thickness distribution graph: 62-layers, H and L on behalf of Ta_2O_5 and SiO_2

3. Experiment

In this experiment, Ta_2O_5 and SiO_2 were deposited on the BK7 glass substrate by using ion beam assisted deposition (IBAD) technique in Leybold coater. IBAD technique had been widely used for improving packing density and atomic mobility of thin films in many applications, especially adopted in optical film industries. Some literatures revealed the optical films with higher and more uniform refractive index for their better packing density and less columnar structure by IBAD [9].

The film deposited by the reasonable deposition rate following the IBAD procedures would also increase the refractive difference and reduce the roughness. According our experimental data, the deposited rate of Ta_2O_5 and SiO_2 are 0.3 and 0.8 nm/s. The chamber was maintained under a vacuum pressure at 1.0×10^{-4} mbar and 1.5×10^{-4} mbar and the oxygen flow was 7 and 20 sccm (standard cubic centimeter per minute). The substrate glass temperature was kept at 200 ˚C.

To fabricate the filter, the thickness errors are expected insensitive for the film . So studying the thickness errors of this filter by scale thickness method and the results were shown in Fig. 4.

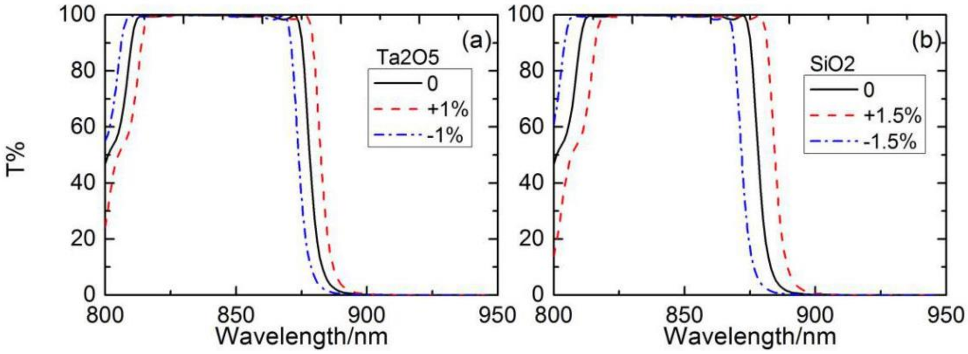

Fig. 4. Showing the thickness error of Ta_2O_5 and SiO_2

From Fig. 4(a), it is shown that when the thickness error of Ta_2O_5 is ±1%, the theoretical transmission curve of the filter will shift ±4 nm. At the same time, when the thickness error of SiO_2 is ±1.5%, the curve will shift ±6 nm. It was deduced that the spectral performance of the design would be sensitive to layer thickness. And such thickness error will cause the filter no longer meet the requirement of the filter. In addition, the layer thickness which was controlled by quartz crystal thickness monitoring achieves maximum accuracy of about 1%~2%[10]. Obviously, the main challenge of depositing the filter is how to control the layer thickness in the process of deposited. Therefore, the indirect monochromatic optical monitor was used to control the layer thickness, and a quartz crystal monitor was utilized to determine the deposited rate.

In this works, proper monitoring wavelength was selected for one monitoring chip, and using one monitoring chip to monitor 6 layers. According to experiments, we used 10 monitoring chips to monitor the film. The method to choose the monitoring wavelength is that the monitoring signal of each layer should pass at least one extrema and the difference between the termination signal level and previous signal extrema is in the range of 10%~60%.

4. Results and discussion

Using Cary 5000 spectrophotometer to measure the spectral performance of the prepared filter at 28.8˚, 30˚ and 31.2˚. Fig. 5(a), (b) and (c) show the transmission curve for average, p- and s-polarized light of the filter when the light is incident upon the film at 28.8˚, 30˚ and 31.2˚ respectively. The results show that high transmittance (>95%) in transmission region and high reflectance (>99.3%) in reflection region, which meet the need of optical-fiber communication system.

As described in section 2, the main effect that increasing the incident angle will lead to blue shift of the transmission curve. When the incident angle is changed from 28.8˚ to 31.2˚, the transmission curves shifts about 6 nm.

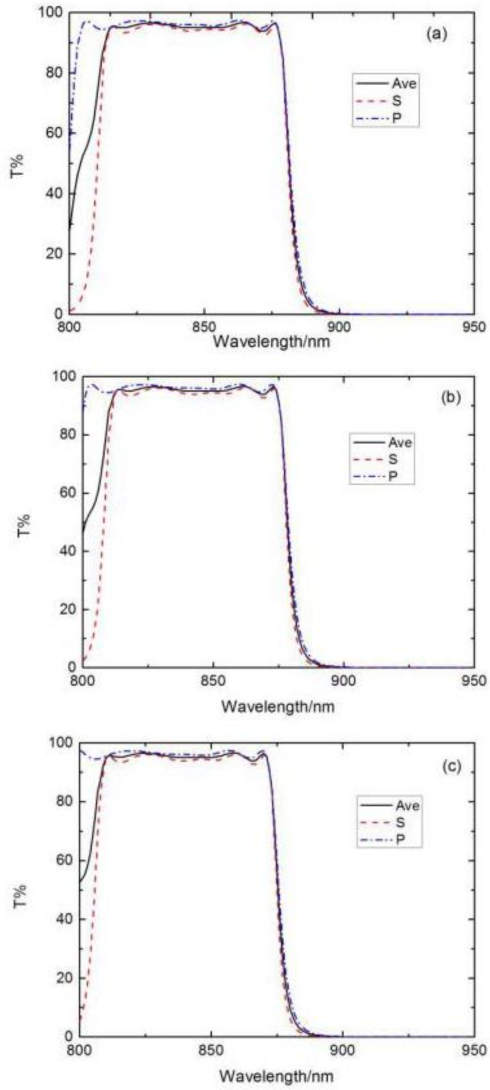

Fig. 5. The transmission curve of the prepared filter at different incident angle

Although the proposed filter presents excellent optical performance, there are still some deviations between theoretical and experimental. According to using reverse engineering method to analysis the test and theoretical simulation data, it can be deduced that these deviations are mainly caused by the mismatching between the substrate and stack.

5. Conclusion

A new kind of symmetrical film system structure sub|(αLHαL)^s|air is proposed to design polarization-independent long-wavelength cutoff filter, which is well demonstrated by simulation and experiments. In experiments, evaporation with IBAD technology and Leybold coater technology are used to fabricate this filter. The most important feature of the prepared filter is that it realizes depolarization. At the same time, it possesses high and smooth transmission curve in the transmission region, and high reflectivity in the cut-off region. These excellent features greatly increase the application range of cutoff filters, and these design methods also bring convenience to the design of optical devices.

Acknowledgment

This research was supported by a grant from the Major Scientific and Technological Projects of Jilin Province (No. 20140203002GX).

References

[1] P. Ma, F. Lin, J. A. Dobrowolski, Applied Optics **50**, C201 (2011).
[2] S. Li, L. Gao, S. Liu, et al., Chinese Optics Letters **12**, 053102 (2014).
[3] H. Qi, R. Hong, K. Yi, J. Shao, Z. Fan, Applied Optics **44**, 2343 (2005).
[4] Q. Cai, H. Luo, Y. Zheng, D. Liu, Optics Express **21**, 19163 (2013).
[5] P. Gu, Z. Zheng, Journal of Zhejiang University-Science A **7**, 1037 (2006).
[6] Xiu-hua Fu, Shi-fu Xiong, Yang Kou, Yong-gang Pan, Heng Chen, Zeng-yu Li, Chuan-xin Zhang Proc. SPIE 9281, 7th International Symposium on Advanced Optical Manufacturing and Testing Technologies: Advanced Optical Manufacturing Technologies 92812D (2014).
[7] A. V. Tikhonravov, M. K. Trubetskov, G. W. DeBell, Applied Optics **46**, 704 (2007).
[8] X. Fu, Y. Kou, D. Liu, J. Zhang, H. Zhu, Acta Optica Sinica **34**, 0731001 (2014).
[9] W. J. Liu, C. M. Chen, Y. C. Lai, SPIE **5723,** 273 (2005).
[10] T. Dimitrova, K. Arshak, E. Atanassova, Thin Solid Films **38**, 31 (2001).

*Corresponding author: fuxiuhua@cust.edu.cn